Modern Particle Physics Experiments
Tracking detectors

Aleksander Filip Żarnecki

FACULTY OF PHYSICS
UNIVERSITY OF WARSAW

Lecture 04

March 25, 2022

Tracking detectors

Tracking detectors

Passage of Particles Through Matter

From the point of view of interactions with matter (resulting in their detection) elementary particles can be divided into following categories:

- charged particles
  $\Rightarrow$ ionization losses
- electrons (and positrons)
  $\Rightarrow$ (ionization +) bremsstrahlung $\searrow$
- photons electromagnetic cascade
  $\Rightarrow$ pair creation $\nearrow$
  (photoelectic effect and Compton scattering at lower energies)
- (uncharged) hadrons
  $\Rightarrow$ hadronic cascade
- neutrinos
  $\Rightarrow$ no direct detection possible

Detector concepts

Depending on the particle type and application, particle detectors can be divided into three main classes:

- Tracking detectors (today)
  Measure position/trajectory of charged particles,
  based on energy losses due to ionization or activation of material.
  We try to minimize particle interactions
  $\Rightarrow$ gaseous detectors or thin semiconductor layers.
- Calorimeters
  Measure particle energy by absorbing it in the dense medium
  Interactions of high energy incident particle
  $\Rightarrow$ electromagnetic or hadronic cascade
- Particle identification detectors
  Use different processes to improve particle identification capabilities
  Cherenkov detectors, Transition radiation detectors, Time-Of-Flight ...

References

- Particle Physics Reference Library (vol.2)
  Review of the state of the art in detector physics and related data-taking technology (open access)

- PDG reviews:
  - Passage of particles through matter
  - Particle detectors at accelerators
  - Particle detectors for non-accelerator physics

Tracking detectors

Maximum energy transfer

Maximum energy transfer to an electron in a single collision

Elastic scattering

Consider elastic scattering of projectile of mass m_1 and energy E_1 on target at rest with mass m_2.

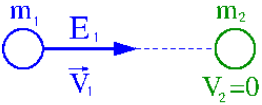

What is the maximum energy transfer possible?

In the CMS frame, maximum transfer corresponds to target (m_2) scattering in the "forward" direction.

Assume parameters of transformation to CMS are known: $\gamma^\star$ and $\beta^\star$

Energy i momentum of m_2 in CMS $(c \equiv 1)$ before collision:

$$
\begin{aligned}
p_2^\star &= -\beta^\star\gamma^\star m_2 \\
E_2^\star &= \gamma^\star m_2
\end{aligned}
$$

after elastic collision:

$$
\begin{aligned}
p'^\star_2 &= -p_2^\star = \beta^\star\gamma^\star m_2 \\
E'^\star_2 &= E_2^\star = \gamma^\star m_2
\end{aligned}
$$

Transforming back to LAB frame:

$$
\begin{aligned}
E'_2 &= \gamma^\star \cdot E'^\star_2 + \beta^\star\gamma^\star \cdot p'^\star_2 \\
&= {\gamma^\star}^2(1+{\beta^\star}^2)m_2
\end{aligned}
$$

Maximum energy transfer

Resulting energy transfer:

$$\Delta E_{max} = E_2' - E_2 = E_2' - m_2$$
$$= \gamma^{\star 2}\left(1 + \beta^{\star 2} - \frac{1}{\gamma^{\star 2}}\right) m_2$$
$$= 2\,(\beta^\star\gamma^\star)^2\, m_2$$

Considered two body system in LAB:

$$E = E_1 + E_2 = E_1 + m_2$$
$$P = P_1 = \sqrt{E_1^2 - m_1^2}$$
$$M^2 = E^2 - P^2 = (E_1 + m_2)^2 - P_1^2$$
$$= m_1^2 + m_2^2 + 2\,E_1\,m_2$$

CMS frame transformation

$$\beta^\star\gamma^\star = \frac{P}{M} = \frac{\beta\gamma m_1}{\sqrt{m_1^2 + 2\gamma m_1 m_2 + m_2^2}}$$

where: γ i β - parameters for m_1

Maximal energy transfer:

$$\Delta E_{max} = \frac{2\,\beta^2\gamma^2\,m_2}{1 + 2\gamma\,\frac{m_2}{m_1} + \left(\frac{m_2}{m_1}\right)^2}$$

For $m_1 \gg m_2$ maximal energy transfer increases as $\beta^2\gamma^2 \sim p_1^2$

$$\Delta E_{max} \approx 2\,\beta^2\gamma^2\,m_2$$

(low energy limit: $m_1 \gg 2\gamma m_2$)

Maximum energy transfer Jupiter notebook 04_Ionisation.ipynb

Maximum energy transfer from proton $(m_p = 938.272081 \text{ MeV})$
to electron $(m_e = 0.51099895 \text{ MeV})$ $(c \equiv 1)$
as a function of momentum:

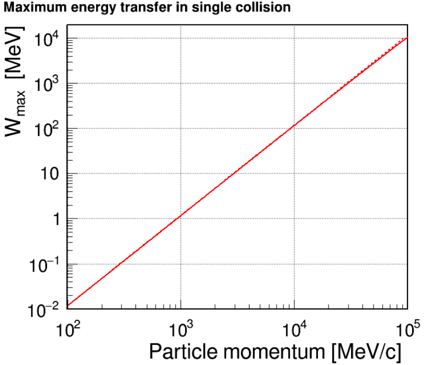

Low energy approximation:

$W_{max} \sim p_p^2$

Maximum energy transfer Jupiter notebook 04_Ionisation.ipynb

Maximum energy transfer from muon ($m_p = 105.6583745$ MeV)
to electron ($m_e = 0.51099895$ MeV) ($c \equiv 1$)
as a function of momentum:

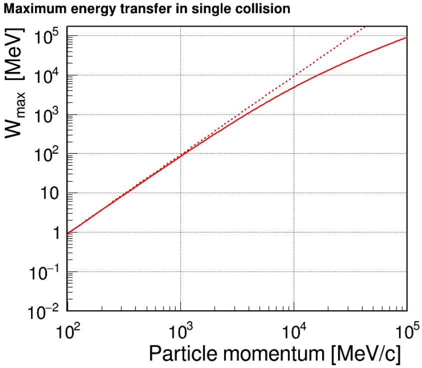

Higher transfer possible for lighter particle (higher $\beta\gamma$)

Low energy approximation (dashed line) no longer valid

Energy transfer in single collision — classical approximation (Bohr)

Heavy $(M \gg m_e)$ charged particle passes electron at rest in a distance b:

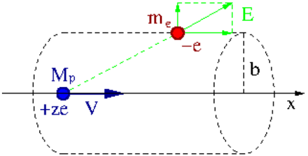

We assume:

- projectile velocity changes can be neglected
- electron displacement can be neglected

Final momentum transfer depends on perpendicular field only:

$$\Delta\vec{p} = \int dt\vec{F} = e\int dt\,\vec{E}_\perp$$

$$\Delta p = e\int dtE_\perp = e\int dx\,\frac{dt}{dx}E_\perp$$

$$= \frac{e}{2\pi b\,V}\int 2\pi b\,dx\,E_\perp$$

From the Gauss law for charge ze:

$$\int dS\,E_\perp = \frac{z\,e}{\varepsilon_0} \quad \Rightarrow \quad \Delta p = \frac{2\,z\,e^2}{4\pi\varepsilon_0\,b\,V}$$

$$\Rightarrow \quad \Delta E(b) = \frac{\Delta p^2}{2m_e} = \frac{2\,z^2\,e^4}{(4\pi\varepsilon_0)^2\,m_e\,b^2\,V^2}$$

Energy transfer in single collision

04_Ionisation.ipynb (2)

Energy transfer from proton with momentum 1000 MeV/c to electron at rest, as a function of impact parameter b:

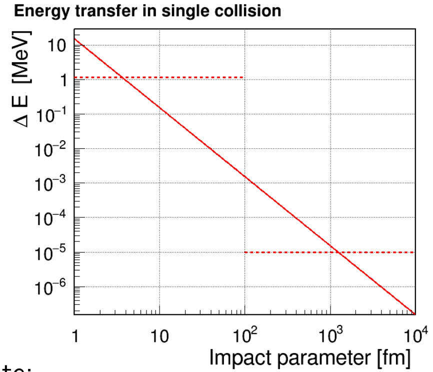

Dashed lines indicate:

- maximum momentum transfer (calculated previously)
- ionization energy level (10 eV) resulting in low-energy cut-off

Average energy loss

After integrating over impact parameter, taking into account electron density in target material (n_e), expected energy loss per unit length is:

$$-\frac{dE}{dx} \quad = \quad \frac{4\pi\ z^2\ \alpha^2\ n_e}{m_e\ V^2} \cdot \log \frac{b_{max}}{b_{min}}$$

Average energy loss

After integrating over impact parameter, taking into account electron density in target material (n_e), expected energy loss per unit length is:

$$-\frac{dE}{dx} \quad = \quad \frac{4\pi \; z^2 \; \alpha^2 \; n_e}{m_e \; V^2} \cdot \log \frac{b_{max}}{b_{min}}$$

We can replace ratio of impact parameters by energy ratio $\Delta E(b) \sim b^{-2}$

$$-\frac{dE}{dx} \quad = \quad \frac{4\pi \; z^2 \; \alpha^2 \; n_e}{m_e \; V^2} \cdot \frac{1}{2} \log \frac{\Delta E_{max}}{\Delta E_{min}}$$

Average energy loss

After integrating over impact parameter, taking into account electron density in target material (n_e), expected energy loss per unit length is:

$$-\frac{dE}{dx} = \frac{4\pi\, z^2\, \alpha^2\, n_e}{m_e\, V^2} \cdot \log \frac{b_{max}}{b_{min}}$$

We can replace ratio of impact parameters by energy ratio $\Delta E(b) \sim b^{-2}$

$$-\frac{dE}{dx} = \frac{4\pi\, z^2\, \alpha^2\, n_e}{m_e\, V^2} \cdot \frac{1}{2} \log \frac{\Delta E_{max}}{\Delta E_{min}}$$

Relating electron density to atomic number:

$$-\frac{dE}{dx} = \frac{4\pi\, N_A\, \alpha^2}{m_e\, c^2} \cdot \rho\, z^2\, \frac{Z}{A} \cdot \frac{1}{\beta^2} \cdot \frac{1}{2} \log \frac{\Delta E_{max}}{\Delta E_{min}}$$

Average energy loss

04_Ionisation.ipynb (3)

Using low energy approximation for ΔE_{max}

$$-\frac{dE}{dx} = \frac{4\pi \; N_A \; z^2 \; \alpha^2}{m_e \; c^2} \cdot \rho \; z^2 \; \frac{Z}{A} \; \frac{1}{\beta^2} \cdot \log\left(\frac{2 \; \beta^2 \gamma^2 \; m_e}{\Delta E_{min}}\right)$$

Assuming ΔE_{min} is given by the ionization energy I (set to 10 eV):

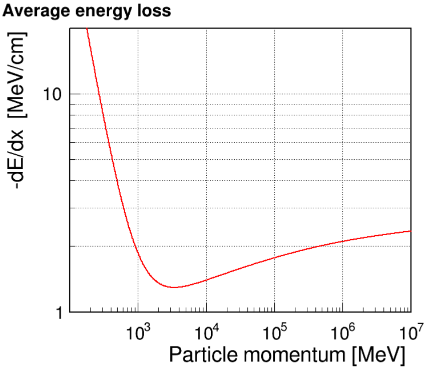

Classical approximation, not very accurate, but qualitative picture correct:

- low β: the faster the particle, the shorter interaction time $\Rightarrow$ lower force impulse
- $\beta \to 1$: logarithmic increase given by increase of the maximum energy transfer

Average energy loss

Bethe-Bloch formula

Taking into account quantum corrections:

$$-\frac{1}{\rho}\frac{dE}{dx} = K \cdot z^2 \frac{Z}{A}\frac{1}{\beta^2}\left[\frac{1}{2}\log\frac{2m_e\beta^2\gamma^2\Delta E_{max}}{I^2} - \beta^2 - \frac{\delta}{2}\right]$$

where: $$K = \frac{4\pi\, N_A\, \alpha^2}{m_e c^2} \approx 0.307\,\frac{MeV}{g/cm^2}$$

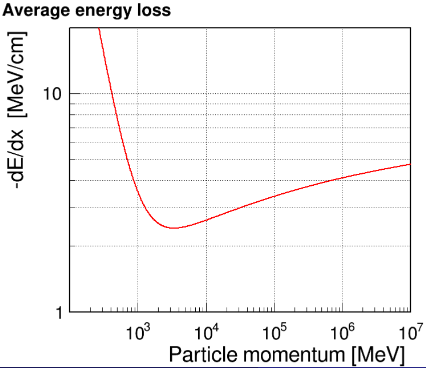

δ - density correction related to medium polarisation

Average energy loss depends mainly on $\beta\gamma$

very weak dependence on projectile mass (only via ΔE_{max})

Average energy loss (PDG)

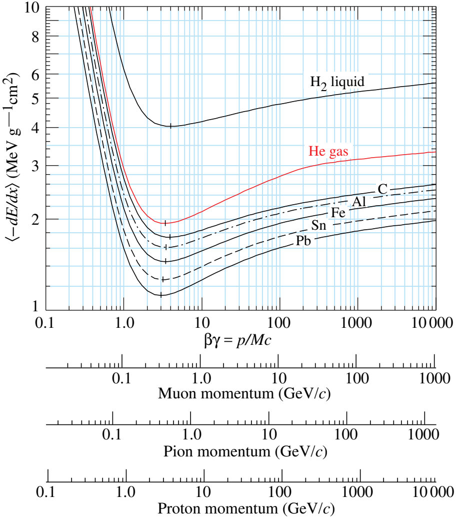

Universal shape of the dependence for different particles!

Scales with $\beta\gamma = p/M$.

Average loss depends on $\beta\gamma$ and medium properties

Minimal ionization for $\beta\gamma \sim 3$
- below: fast rise
- above: logarithmic rise

For minimum ionizing particle (MIP): $-\frac{dE}{dx}\Big|_{min} \sim 1 - 2 MeV / \frac{g}{cm^2}$

Average energy loss (PDG)

Minimum ionization loss (per unit density) for different elements:

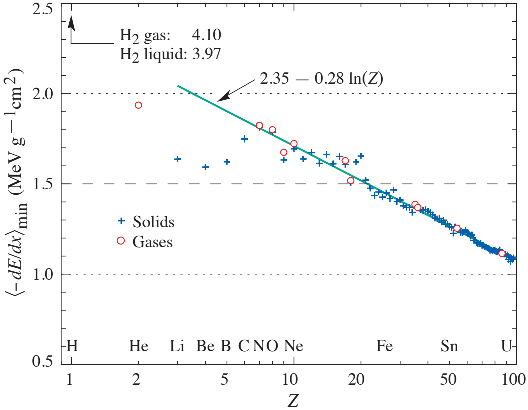

Highest ionization losses for hydrogen, for $Z > 6$ decreases with $\log(Z)$.

$\sim 2.2 MeV / \frac{g}{cm^2}$ for water (liquid)

Mean energy loss

Average energy loss (PDG)

Muon energy losses as a function of momentum

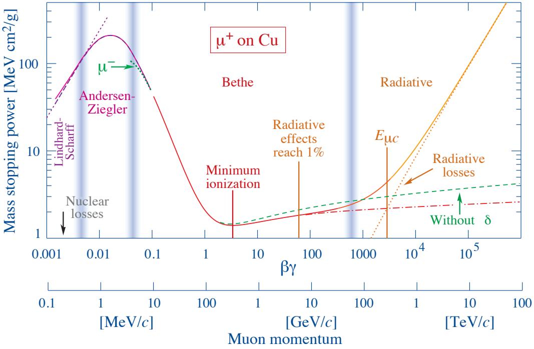

Bethe-Bloch formula is not valid for:

$\beta < 0.05$: electron binding energy and motion, as well as particle scattering can not be neglected

$\beta\gamma > 300$ (for muons): radiative losses become important

For muons, Bethe-Bloch formula gives correct energy loss estimate for muon momenta from about 10 MeV to 30 GeV

Above 100 GeV (LHC, IceCube) radiative losses can become important

Bragg peak

Consider beam of protons with kinetic energy E_k=300 MeV entering the volume filled with liquid water.

Calculate (and plot) the ionization energy loss distribution along the proton path, as a function of the propagation distance in water. (use numerical integration)

Compare the expected proton range in water for E_k=100 MeV, 200 MeV, 300 MeV and 400 MeV.

What is the energy range useful for medical therapy?

Tracking detectors

Landau distribution

04_Landau.ipynb (1)

Bethe-Bloch equation describes average ionization losses.

For detectors with moderate thickess, the energy loss probability distribution is adequately described by the Landau distribution.

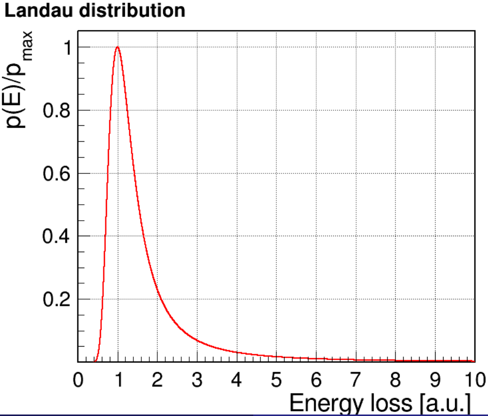

Implemented in ROOT:
TMath::Landau()

(scaled and shifted for maximum at 1)

Landau distribution

04_Landau.ipynb (2)

Also integrated distribution implemented in ROOT

⇒ can be used for event generation:

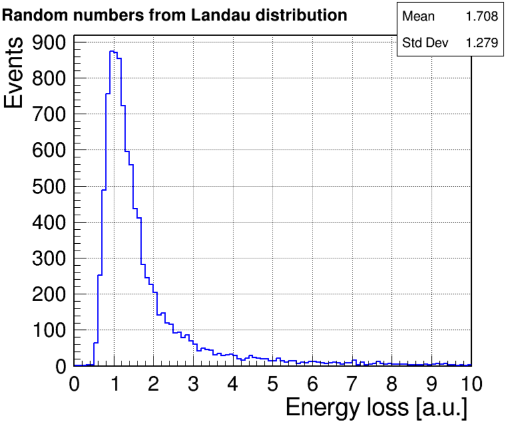

Landau distribution 04_Landau.ipynb (2)

Also integrated distribution implemented in ROOT

⇒ can be used for event generation:

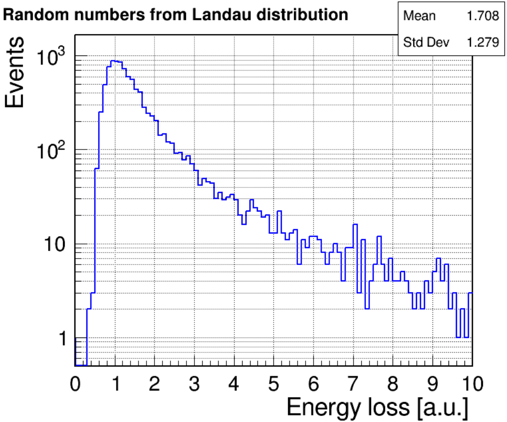

Very significant tail of the distribution!

Mean value from all 10000 entries: 4.806 (Std Dev: 125.08) !!!

Landau distribution

04_Landau.ipynb (3)

Bethe-Bloch formula: average of truncated Landau distribution (ΔE_{max}).

In the limit $\beta\gamma \to \infty$ ($\Delta E_{max} \to \infty$), mean and RMS of the energy loss distribution are not well defined! But the most probable value is...

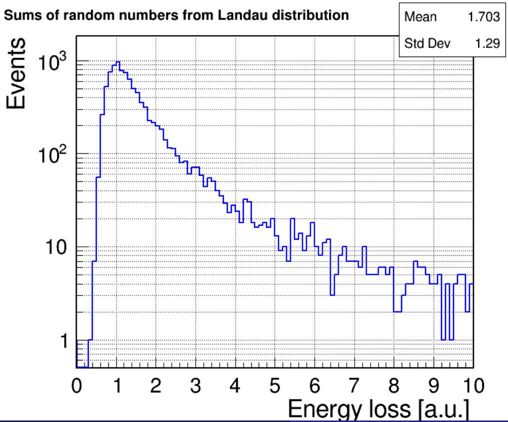

single deposit $\Rightarrow \frac{\sigma}{Mean} \approx 0.76$

(from histogram range $\sim 10 \cdot x_{max}$)

Landau distribution

04_Landau.ipynb (3)

Bethe-Bloch formula: average of truncated Landau distribution (ΔE_{max}).

In the limit $\beta\gamma \to \infty$ ($\Delta E_{max} \to \infty$), mean and RMS of the energy loss distribution are not well defined! But the most probable value is...

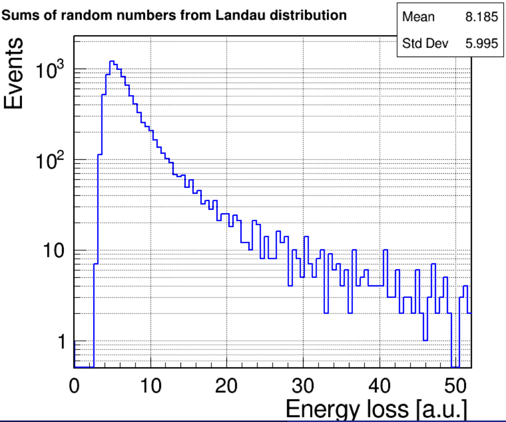

Sum of Landau distributed deposits is also described by Landau distribution!

$$N_{sum} = 4 \Rightarrow \frac{\sigma}{Mean} \approx 0.73$$

(from histogram range $\sim 10 \cdot x_{max}$)

Landau distribution

04_Landau.ipynb (3)

Bethe-Bloch formula: average of truncated Landau distribution (ΔE_{max}).

In the limit $\beta\gamma \to \infty$ ($\Delta E_{max} \to \infty$), mean and RMS of the energy loss distribution are not well defined! But the most probable value is...

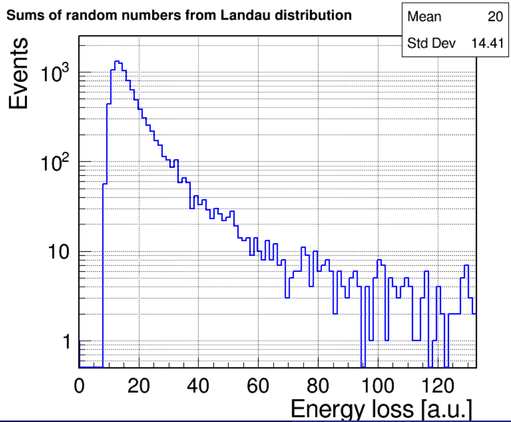

Sum of Landau distributed deposits is also described by Landau distribution!

$$N_{sum} = 9 \Rightarrow \frac{\sigma}{Mean} \approx 0.72$$

(from histogram range $\sim 10 \cdot x_{max}$)

Landau distribution

04_Landau.ipynb (3)

Bethe-Bloch formula: average of truncated Landau distribution (ΔE_{max}).

In the limit $\beta\gamma \to \infty$ ($\Delta E_{max} \to \infty$), mean and RMS of the energy loss distribution are not well defined! But the most probable value is...

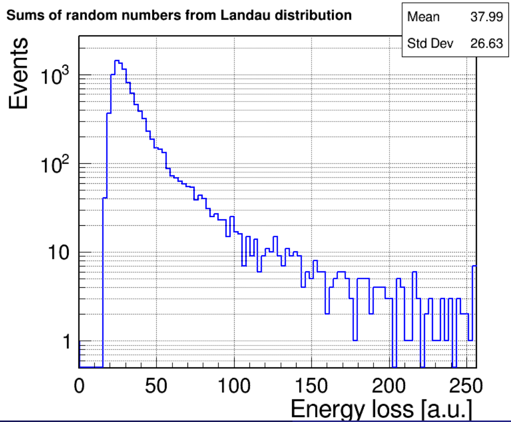

Sum of Landau distributed deposits is also described by Landau distribution!

$$N_{sum} = 16 \Rightarrow \frac{\sigma}{Mean} \approx 0.70$$

(from histogram range $\sim 10 \cdot x_{max}$)

Landau distribution

04_Landau.ipynb (3)

Bethe-Bloch formula: average of truncated Landau distribution (ΔE_{max}).

In the limit $\beta\gamma \to \infty$ ($\Delta E_{max} \to \infty$), mean and RMS of the energy loss distribution are not well defined! But the most probable value is...

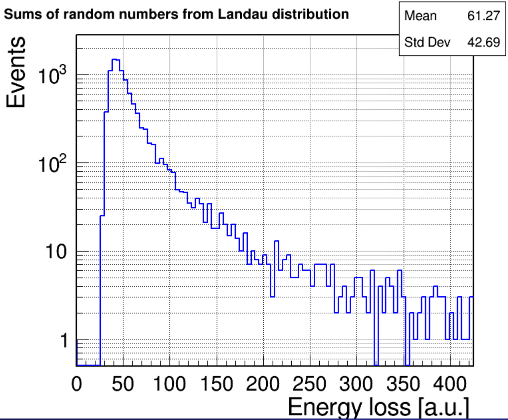

Sum of Landau distributed deposits is also described by Landau distribution!

$$N_{sum} = 25 \Rightarrow \frac{\sigma}{Mean} \approx 0.69$$

(from histogram range $\sim 10 \cdot x_{max}$)

Landau distribution

04_Landau.ipynb (3)

Bethe-Bloch formula: average of truncated Landau distribution (ΔE_{max}).

In the limit $\beta\gamma \to \infty$ ($\Delta E_{max} \to \infty$), mean and RMS of the energy loss distribution are not well defined! But the most probable value is...

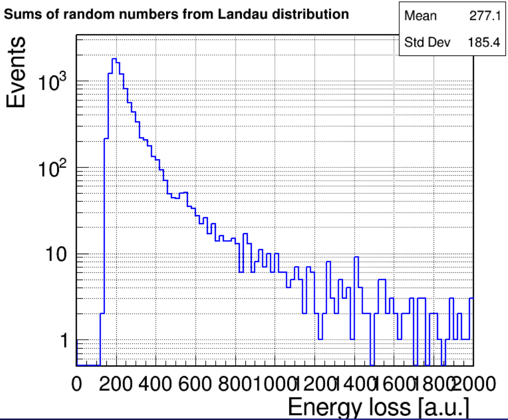

Sum of Landau distributed deposits is also described by Landau distribution!

$$N_{sum} = 100 \Rightarrow \frac{\sigma}{Mean} \approx 0.67$$

(from histogram range $\sim 10 \cdot x_{max}$)

Landau distribution

04_Landau.ipynb (3)

Bethe-Bloch formula: average of truncated Landau distribution (ΔE_{max}).

In the limit $\beta\gamma \to \infty$ ($\Delta E_{max} \to \infty$), mean and RMS of the energy loss distribution are not well defined! But the most probable value is...

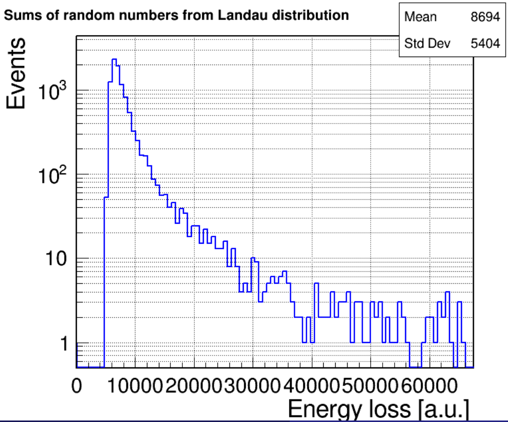

Sum of Landau distributed deposits is also described by Landau distribution!

$$N_{sum} = 2500 \Rightarrow \frac{\sigma}{Mean} \approx 0.62$$

(from histogram range $\sim 10 \cdot x_{max}$)

High energy tail significant even in large detector volumes!

Landau distribution (PDG)

Mean energy loss is a subject of very large fluctuations $(\Delta E_{max} \gg \langle \Delta E \rangle)$

It is much more convenient to consider most probable loss value (MPV).

In the limit $\beta\gamma \to \infty$ $(\Delta E_{max} \to \infty)$, MPV $\to$ constant!

MPV for 500 MeV pion in silicon

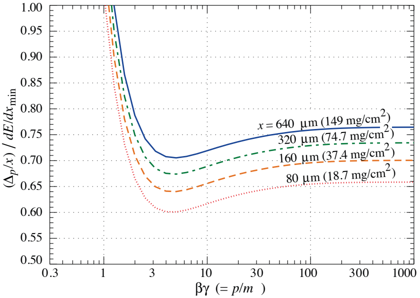

Ionization losses in ALICE TPC

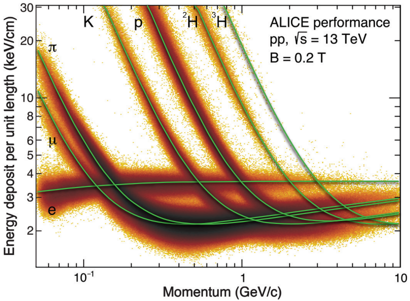

Tracking detectors

Ionization in gases

Long tail in Landau distribution ⇒ secondary ionization very important
Total ionization (N_T) is 2–3 time higher than the primary one (N_P)!

Primary and total number of electron-ion pairs per cm, for unit charge MIP (in normal conditions)

Gas	N_P	N_T
H_2	5.2	9.2
Ne	13	40
Ar	25	97
Xe	41	312
CH_4	28	54
CO_2	35	100

However, these are extremely small charges: $312\,e \approx 0.05\,\mathrm{fC}$
We are not able to measure them directly...

Ionization in gases

Measurement of the corresponding current is not possible, unless we apply electric field strong enough to create an electron avalanche.

Electron drifting in gas get sufficient energy (between two subsequent collisions) to ionize.

First Townsend ionisation coefficient gives the number of ion pairs generated per unit length

$$dn = \alpha \cdot n_{\circ}\, dx$$

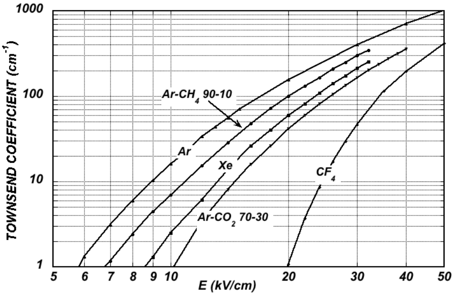

Charge multiplication is crucial!

We need to amplify the signal to the level that can be measured with dedicated electronics...

Ionization in gases

Measurement of the corresponding current is not possible, unless we apply electric field strong enough to create an electron avalanche.

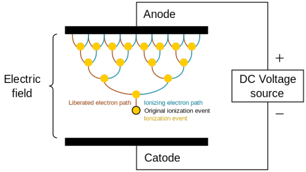

In the uniform field we are not able to obtain large multiplication factors (in the proportional mode).

Ionization in gases

Measurement of the corresponding current is not possible, unless we apply electric field strong enough to create an electron avalanche.

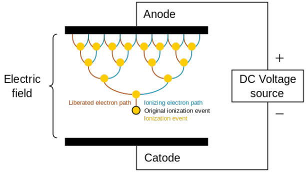

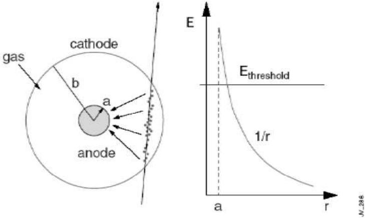

In the uniform field we are not able to obtain large multiplication factors (in the proportional mode).

Strong electric field resulting in large multiplication can be easily obtained around the thin anod wire.

Detected charge is still very low, but can be measured with sensitive electronics. Charge multiplication is crucial...

Principles of operation

Simplest counter design - single wire (like in Geiger-Müller tube)

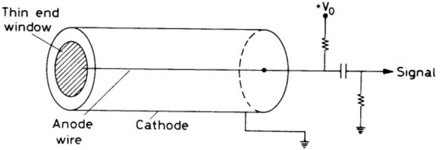

We can measure the charge flow (current) on anode wire and on cathode surface!

Cathod readout allows for additional segmentation
⇒ better position measurement

Counter performance depends on the voltage applied

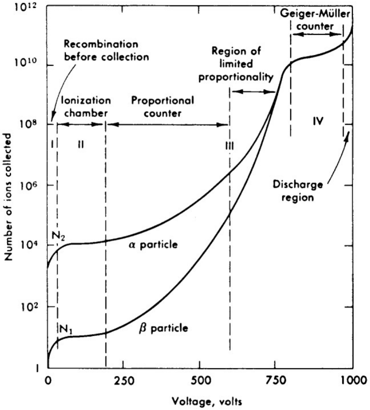

Proportional mode allows for measurement of primary ionization

Multiwire proportional chamber (MWPC)

Georges Charpak 1970
(Nobel 1992)

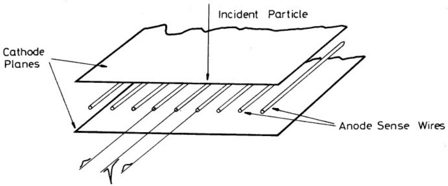

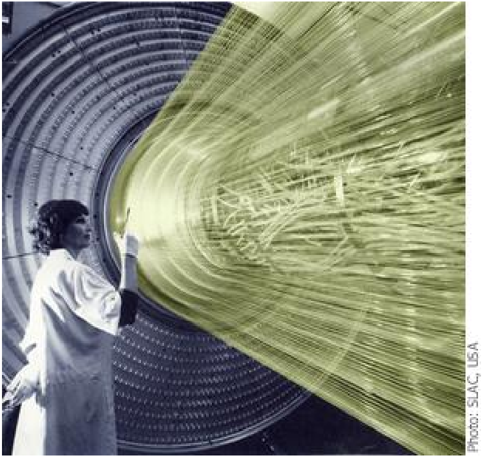

Simple and Cheap!
Can be used to cover large surfaces

First detector allowing for fully electronic readout!
$\Rightarrow$ revolution in HEP

Multiwire proportional chamber (MWPC)

Georges Charpak 1970
(Nobel 1992)

Charge induced on segmented cathods
⇒ 2-D position reconstruction possible

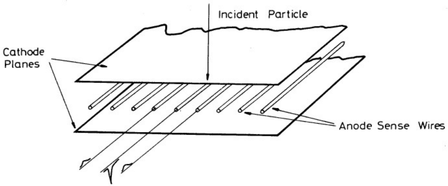

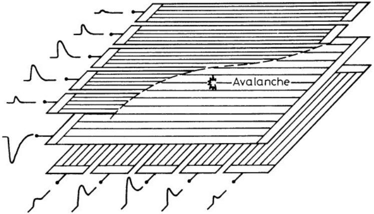

Simple and Cheap!
Can be used to cover large surfaces

First detector allowing for fully electronic readout!
⇒ revolution in HEP

Charge sharing between strips
⇒ position reconstruction precision higher than readout segmentation

Micro Strip Gas Chamber (MSGC)

Wires are the “weak point” of MWPC
they can not be put to close to each other, they break easily...

One can replace wires with narrow strips:

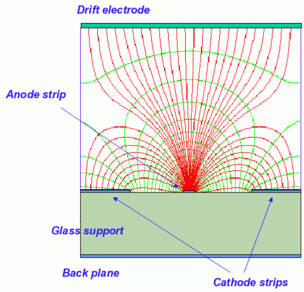

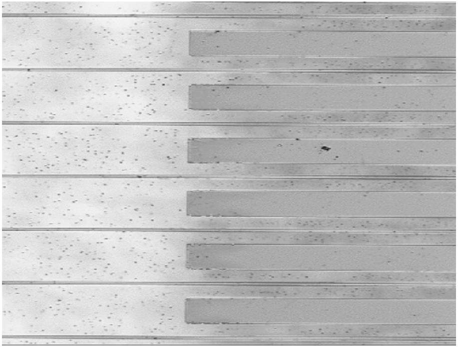

Micro Strip Gas Chamber (MSGC)

Wires are the "weak point" of MWPC
they can not be put to close to each other, they break easily...

One can replace wires with narrow strips:

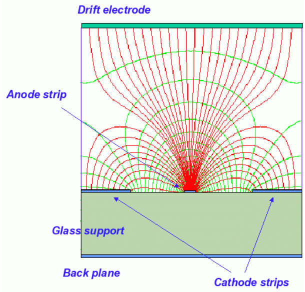

Higher "wire" density allows for higher detection rate:

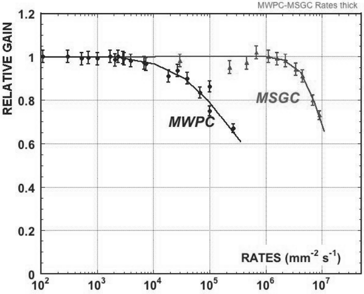

Micromegas

Even higher readout strip density possible, if gas amplification only in restricted region:

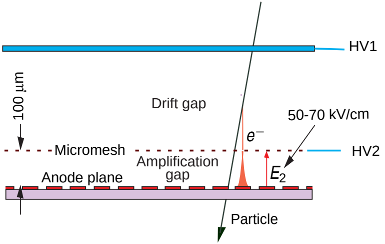

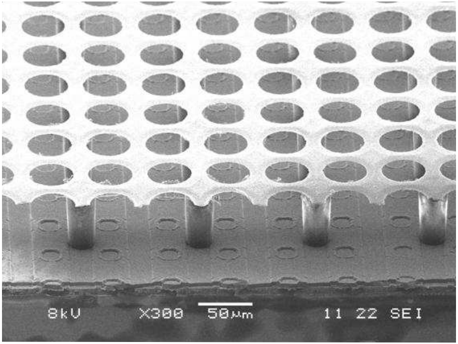

excellent spatial resolution $\mathcal{O}(10)\,\mu m$, very fast signals

no problem with space-charge accumulation (ions) $\Rightarrow$ high rates possible

Gas Electron Multiplier (GEM)

Multiple small holes in copper-insulator-copper foil

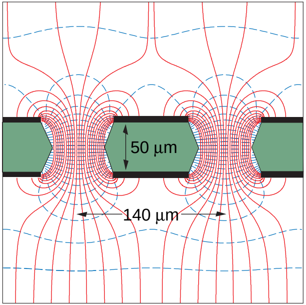

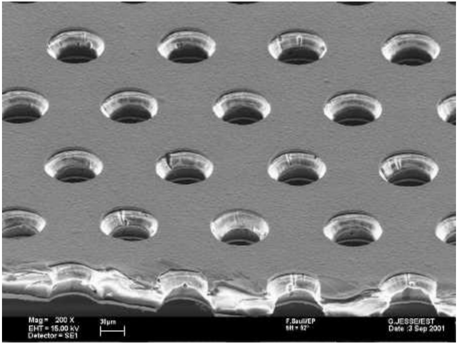

potential difference ⇒ electric field
⇒ each hole acts as an independent proportional counter

Gas Electron Multiplier (GEM)

Multiple small holes in copper-insulator-copper foil

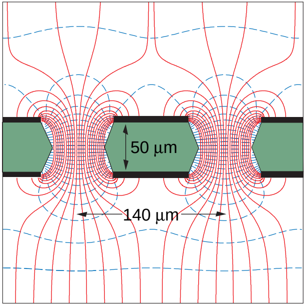

potential difference ⇒ electric field
⇒ each hole acts as an independent proportional counter

Even higher gain can be obtained when using multiple GEM foils:

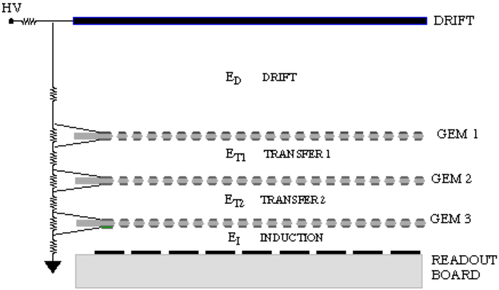

Resisitve Plate Chambers (RPC)

Single gap RPC:
modern "spark chamber"

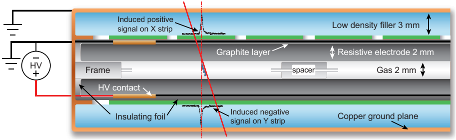

very high field ⇒ discharge mode (!)
resistive electrodes ⇒ local discharge only

ideal for covering very large surfaces
(muon systems of ATLAS and CMS)

Multiple gap RPC (mRPC)

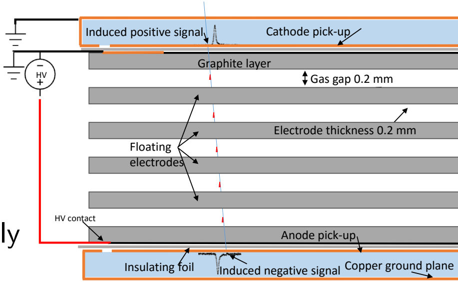

Much better timing resolution
(down to 20 ps !)

Electron drift velocity

Unless gas layer is very thin, electron drift time has to be taken into account. Finite drift velocity contributes to signal delay and time spread.

Drift velocity strongly depends on the gas mixture, electric and magnetic field:

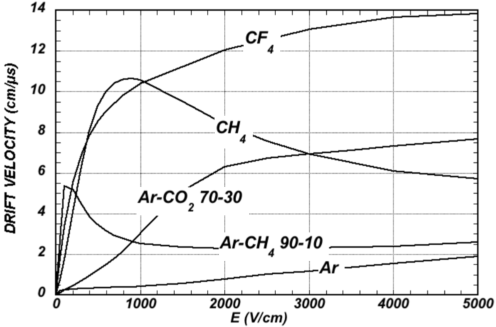

We can use signal delay to reconstruct position of the primary ionization!
Many different detector designs are used...

Time Projection Chamber (TPC) invented in the 1970's

Ionization electrons drift in a uniform electric field towards amplification layer with 2-D position readout

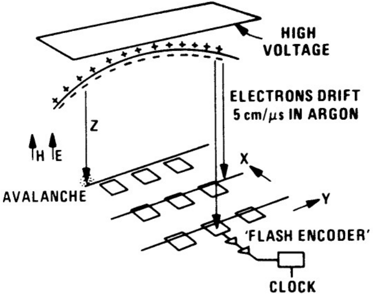

⇒ Z reconstructed from drift time

Schematic view of the ALICE TPC

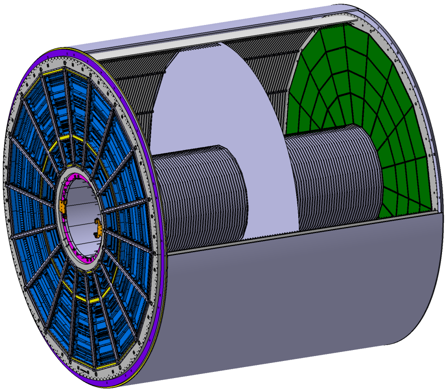

Amplification stage based on GEMs

Time Projection Chamber (TPC)

Examples of reconstructed events:

STAR @ RHIC

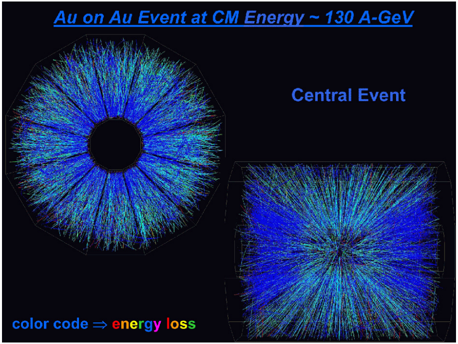

NA49 @ CERN SPS

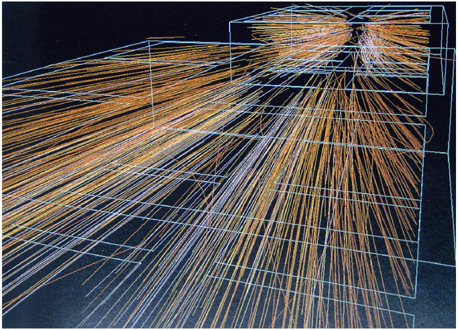

Measurement of ionization loss allows for (partial) particle identification

see pg. 24